# Isotopic constraints on carbon exchange between deep ocean sediments and sea water

**James E. Bauer*, Clare E. Reimers†, Ellen R. M. Druffel‡ & Peter M. Williams§**

* School of Marine Science, College of William and Mary, Gloucester Point, Virginia 23062-1346, USA
† Institute of Marine and Coastal Sciences, Rutgers University, New Brunswick, New Jersey 08903-0231, USA
‡ Department of Earth System Science, University of California, Irvine, California 92717, USA
§ Marine Research Division, Scripps Institution of Oceanography, University of California, San Diego, La Jolla, California 92093-0128, USA

**THE vast reservoirs of organic carbon in marine sediments[1–3] have the potential to influence the properties of organic matter in the overlying water column. For example, it has been suggested that marine sediments are a possible source of the old, refractory dissolved organic carbon (DOC) found in deep water[3,4]. Natural radiocarbon and stable carbon isotope ratios ($\Delta^{14}C$ and $\delta^{13}C$) can be used to constrain the role of sediments in the ocean carbon cycle[5–8]. Here we report the distributions of $\Delta^{14}C$ and $\delta^{13}C$ associated with dissolved organic and inorganic carbon in sediment pore water, together with those of the particulate sedimentary organic carbon, from two geochemically distinct marine environments. Concentration gradients of dissolved organic and inorganic carbon across the sediment–water interface imply significant diffusive fluxes of these solutes from the sediment to the water column. But the DOC fraction in the sediments is greatly enriched in $^{14}C$ compared with that in the overlying sea water (by as much as 370‰), indicating that the DOC supplied by sediments to ocean waters must be relatively young, and that its remnant ages in the water column itself.**

Sediments were collected from two regions of the eastern North Pacific Ocean. Station N (35° 00′ N, 123° 00′ W) is located in 4,100 m of water on the continental rise at the base of the Monterey deep sea fan[9]. Santa Monica basin (33° 45′ N, 118° 45′ W), a semi-enclosed, nearly anoxic basin in the California continental borderland, has an average mid-basin depth[10] of ~900 m. The $\Delta^{14}C$ values of sedimentary organic carbon (SOC) were highly dissimilar between the two sites (Fig. 1*a*, *b*; Table 1). Relative to modern, pre-bomb, carbon in surface ocean waters ($\Delta^{14}C \approx -70‰$)[11], the SOC of surface sediments at station N was uniformly depleted in $^{14}C$ (average $\Delta^{14}C = -237 \pm 3‰$, $n = 6$, 0–1.5 cm). The $\Delta^{14}C$ values were markedly lower in deeper layers ($-344 \pm 7‰$ at 9.5 cm). In contrast to station N, the SOC from the central Santa Monica basin had a clear post-bomb $^{14}C$ signal ($\Delta^{14}C > -50‰$) to at least 2 cm depth. The steep $\Delta^{14}C$ gradient in SOC ($\Delta^{14}C$-SOC) between ~3 cm depth and the sediment surface at Santa Monica is a result of the increasing global inventory of $^{14}C$ during atmospheric weapons testing of the 1950s and 1960s, while the much lower gradient from ~5–10 cm reflects $^{14}C$ decay over time.

Concentrations of DOC in sea water overlying the sediments ($DOC_{olw}$) of each site were low (~40 μM), and increased to $428 \pm 8$ μM and $453 \pm 8$ μM in surficial (0–0.25 cm depth) pore waters ($DOC_{pw}$) at station N and Santa Monica basin, respectively (Table 1). The $DOC_{pw}$ increased to higher values in the basin (706 μM at 8.5 cm) than in station N (500 μM at 8.5 cm) sediments. This may be due to greater SOC content and anoxia in the former location, leading to greater production but less efficient respiration of $DOC_{pw}$.

There was close agreement between the $\Delta^{14}C$ and $\delta^{13}C$ of SOC and $DOC_{pw}$ in shallow station N sediments (Fig. 1*a*, Table 1). The simplest explanation for this is biotic and abiotic solubilization of SOC to DOC. Particulate organic carbon (POC) sinking from the water column to the sediment surface is comparatively enriched in $^{14}C$ (−39 to +136‰)[5]. Thus the greater similarity of $\Delta^{14}C$-$DOC_{pw}$ to 'average' $\Delta^{14}C$-SOC indicates that $DOC_{pw}$ in station N surface sediments is derived from a mixture of young and old components comprising the bulk SOC rather than from exclusively young, biologically labile POC. The increasing difference between the $\Delta^{14}C$ of $DOC_{pw}$ and SOC with sediment depth may result from long-term diagenetic reactions and differential diffusion of $DOC_{pw}$ components within sediments.

At Santa Monica basin, all $\Delta^{14}C$ values of $DOC_{pw}$ were lower than those of SOC (Fig. 1*b*, Table 1). The greatest difference (~260‰) between the $\Delta^{14}C$ of $DOC_{pw}$ and SOC (similar to sinking POC[5]) was in the shallowest sediment layer (0–0.25 cm), suggesting that $DOC_{olw}$ may diffuse into (or be mixed with) near-surface pore water. We calculate that if surficial pore waters contained $DOC_{olw}$ with an assumed concentration of ~40 μM and $\Delta^{14}C$ of −462‰, the undiluted $DOC_{pw}$ at 0–0.25 cm must have an average $\Delta^{14}C$ of ~ −230‰, close to that observed, but significantly lower than the average bulk $\Delta^{14}C$ of SOC at this depth. The depletion in $^{14}C$ of $DOC_{pw}$ in deep sediments of station N (Fig. 1*a*) and shallow sediments of Santa Monica basin (Fig. 1*b*) may also result from (1) age-fractionated diffusion of $DOC_{olw}$ components into pore waters (the net flux of DOC is out of the sediments) or (2) selective dissolution and enzymatic hydrolysis of SOC fractions[12], coupled with the different pathways of respiration (that is, DOC-utilization) dominating at each site and depth.

The $\delta^{13}C$ values and concentrations of porewater dissolved inorganic carbon ($DIC_{pw}$) in marine sediments reflect contributions from $DOC_{pw}$ and/or SOC mineralization, mixing with DIC from the overlying water column ($DIC_{olw}$), and $CaCO_3$ dissolution[6,8,13,14]. The more rapid changes in $DIC_{pw}$ concentrations and $\delta^{13}C$ values with depth at Santa Monica basin compared to station N indicate that a greater percentage of the porewater DIC at the former location is derived from isotopically light marine organic matter ($\delta^{13}C = \sim -18$ to −22‰) than

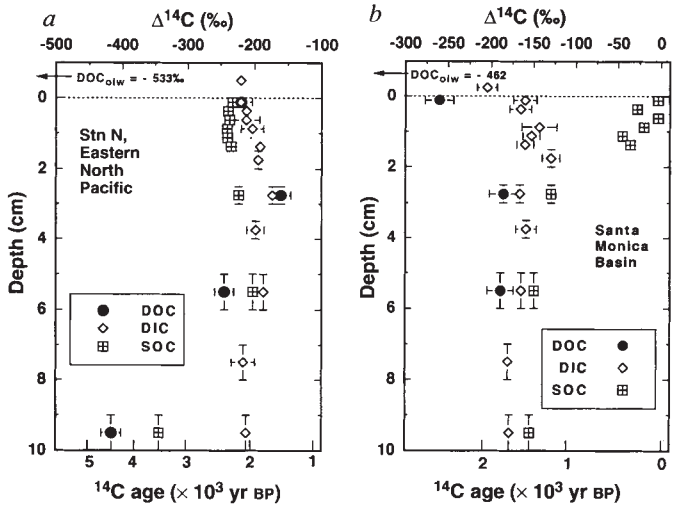


FIG. 1 Depth profiles of $\Delta^{14}C$ signatures of porewater DOC, DIC and solid-phase SOC in sediments from station N in the eastern North Pacific (*a*) and Santa Monica basin (*b*). Vertical bars are depth intervals for each data point. Horizontal bars are $\pm 1\sigma$ of $\Delta^{14}C$ measurement. Symbols without bars have depth intervals or $\sigma$ values smaller than the symbols. $DOC_{olw}$ indicates here $\Delta^{14}C$ values of DOC in sea water overlying sediments (off-scale relative to all other $\Delta^{14}C$ values at both sites). Dashed horizontal lines represent the sediment–water interface. See Table 1 legend for details of sample processing.

TABLE 1 Carbon concentrations and isotopic ratios of DOC, DIC and SOC in pore waters and sediments

| | | DOC | | | DIC | | | SOC | |
|---|---|---|---|---|---|---|---|---|---|
| Site | Depth interval (cm) | μM | $\delta^{13}C$* (‰) | $\Delta^{14}C$† (‰) | μM | $\delta^{13}C$* (‰) | $\Delta^{14}C$† (‰) | $\delta^{13}C$* (‰) | $\Delta^{14}C$† (‰) |
| Stn N | OLW‡ | 40 | −20.8 | −533 | 2,376 | 0.0 | −220 | | |
| | 0–0.25 | 428§ | −21.9 | −220 | 2,432 | −0.2 | −220 | −21.8 | −232 |
| | 0.25–0.5 | | | | 2,394 | −0.1 | −212 | | −239 |
| | 0.5–0.75 | 359 | | | 2,390 | −0.1 | −212 | | −237 |
| | 0.75–1.0 | 279 | | | 2,551 | −0.6 | −203 | | −241 |
| | 1.0–1.25 | 366 | | | 2,500 | −0.6 | | | −240 |
| | 1.25–1.5 | 753 | | | 2,516 | −0.7 | −191 | | −235 |
| | 1.5–2.0 | | | | 2,671 | −1.1 | −194 | | |
| | 2.0–2.5 | 474 | | | | | | | |
| | 2.5–3.0 | 500§ | −20.8 | −161 | 2,761 | −1.5 | −173 | −21.8 | −223 |
| | 3.0–3.5 | 559 | | | | | | | |
| | 3.5–4.0 | | | | 2,769 | −1.7 | −198 | | |
| | 4.0–5.0 | 442 | | | | | | | |
| | 5.0–6.0 | 434§ | −22.1 | −245 | 2,804 | −1.8 | −186 | −21.8 | −202 |
| | 6.0–7.0 | 463 | | | | | | | |
| | 7.0–8.0 | | | | 2,742 | −2.0 | −217 | | |
| | 8.0–9.0 | 495 | | | | | | | |
| | 9.0–10.0 | 508§ | −22.9 | −417 | 2,813 | −2.0 | −212 | −21.9 | −344 |
| SMB | OLW‡ | 42 | −20.8 | −462 | 2,329 | −0.1 | −205 | | |
| | 0–0.25 | 453 | | | | | | | |
| | 0–0.25 | 465§ | −21.2 | −260 | 2,468 | −1.2 | −160 | −21.5 | −4 |
| | 0.25–0.5 | 413 | | | 2,570 | −2.4 | −165 | | −28 |
| | 0.5–0.75 | 551 | | | | | | | −4 |
| | 0.75–1.0 | 546 | | | 2,634 | −2.4 | −144 | | −20 |
| | 1.0–1.25 | 529 | | | 2,665 | −2.7 | −153 | | −45 |
| | 1.25–1.5 | 557 | | | 2,685 | −2.9 | −160 | | −36 |
| | 1.5–2.0 | | | | 2,817 | −3.5 | −130 | | |
| | 2.0–2.5 | 530 | | | | | | | |
| | 2.5–3.0 | 729§ | −21.8 | −186 | 3,133 | −4.6 | −166 | −21.6 | −130 |
| | 3.5–4.0 | | | | 3,300 | −5.4 | −159 | | |
| | 4.0–5.0 | 775 | | | | | | | |
| | 5.0–6.0 | 812§ | −22.5 | −189 | 3,516 | −6.7 | −165 | −22.3 | −150 |
| | 6.0–7.0 | 687 | | | | | | | |
| | 7.0–8.0 | | | | 3,780 | −7.8 | −180 | | |
| | 8.0–9.0 | 706 | | | | | | | |
| | 9.0–10.0 | | | | 4,012 | −8.8 | −179 | −22.2 | −155 |

DOC, dissolved organic carbon; DIC, dissolved inorganic carbon; SOC, sedimentary organic carbon. Surface ocean waters at station N (Stn N) have a summer maximum in primary productivity derived from upwelled nutrients, a fraction of which is exported episodically to the sea floor leading to an increase in surface sediment organic-matter content from June to August[20,21]. A $^{210}Pb$ profile, bottom photography and core X-radiography also demonstrate[9,21,22] that these sediments are highly bioturbated to 5–6 cm depth. Sediments at Santa Monica basin (SMB) have a surface microbial mat that largely consists of iron-oxidizing bacteria; the sediments are laminated, indicating minimal disturbance by bioturbating infauna[10]. Oxygen is depleted by ~3 cm depth at station N and 2–3 mm depth at SMB[22]. The limit of detectable nitrate penetration at both sites is ~3 cm depth[9,23]. Total sediment accumulation rates have been estimated to be 12 mg $cm^{-2}$ $yr^{-1}$ at station N[24] and 14–24 mg $cm^{-2}$ $yr^{-1}$ at SMB[25,26].

METHODS. Subcores from Soutar box cores[9] or gravity cores were sectioned at 0.25-cm intervals over the top 1.5 cm, 0.5-cm intervals from 1.5 to 6 cm, and 1.0-cm intervals at greater depth. All sample processing was performed close to *in situ* temperature under oxygen-free conditions. The potential effects of pressure and temperature changes on sediment organic matter during sample retrieval have been noted, but not evaluated, in previous studies[27] because of limitations in sampling technology. Pore water was separated from bulk sediments by centrifugation at 5,000 r.p.m., a speed which was not found to induce $DOC_{pw}$ sampling artefacts[27], and filtered through pre-combusted glass fibre filters. Subsamples for $DOC_{pw}$ and SOC analyses were immediately frozen at −20 °C. Pore water for DIC analyses was treated with a saturated $HgCl_2$ solution and refrigerated at 4 °C. Detailed profiles of $DOC_{pw}$ concentrations were determined by discrete-injection (50 μl) high-temperature catalytic oxidation (HTCO)[28]. For $\Delta^{14}C$ and $\delta^{13}C$ analyses of $DOC_{pw}$, 10–20 ml samples were acidified to pH 2–2.5 with 10% $H_3PO_4$, sparged free of inorganic carbon, and oxidized to $CO_2$ by continuous-injection HTCO[5,15]. The $DOC_{olw}$ was oxidized by irradiation of 650-ml samples with a 2,400-W ultraviolet light source, and procedural $\Delta^{14}C$-DOC blanks were determined periodically[5,15]. Samples (5–10 ml) for DIC analyses were acidified to pH ~2, and total $CO_2$ was sparged and collected[8]. SOC samples were acidified for 24 h with 3% $H_3PO_4$ to remove carbonates, dried, and combusted to $CO_2$ in sealed quartz tubes at 850 °C (ref. 29). Dry-weight sediment organic and carbonate carbon contents in the uppermost 10 cm were, respectively: station N, 1.5–2% and 0.1–0.2%; SMB, 4.5–5% and 1.3–2.3%; J.E.B., unpublished data). Average measurement errors ($\pm 1\sigma$) for each analysis are: DOC, 8 μM; DIC, ±1 μM; $\delta^{13}C$, ±0.2‰; $\Delta^{14}C$-DOC, ±15‰; $\Delta^{14}C$-DIC, ±12‰; $\Delta^{14}C$-SOC, ±7‰.

* $\delta^{13}C = ([R_{sample}/R_{standard}] - 1) \times 1{,}000$, where $R = {}^{13}C/{}^{12}C$ as measured by isotope-ratio mass spectrometry.

† $\Delta^{14}C$ is defined as the deviation in parts per thousand from the $^{14}C$ activity of nineteenth-century wood and is calculated in the conventional manner[30]. All $\Delta^{14}C$ analyses were made at the Center for Accelerator Mass Spectrometry, Lawrence Livermore National Laboratory, on total amounts ranging from ≤100 μg (DOC) to ~1,000 μg (DIC, SOC) of carbon following the conversion of sample $CO_2$ to graphite targets[31].

‡ OLW, values for DOC and DIC in sea water overlying sediments at each site.

§ $DOC_{pw}$ concentrations determined by continuous-injection HTCO during processing of $\Delta^{14}C$ and $\delta^{13}C$ samples. All reported DOC concentrations and $\Delta^{14}C$ and $\delta^{13}C$ values were corrected by the corresponding system blanks (~3–5 μM C for discrete injection; 0.2 μmol C for continuous injection[5,15,28]).

TABLE 2 Calculated and measured fluxes of DOC and DIC

| Site | Calculated fluxes DOC ($g\,C\,m^{-2}\,yr^{-1}$) | Calculated fluxes DIC | Measured fluxes DIC ($g\,C\,m^{-2}\,yr^{-1}$) | Source of measured flux |
|---|---|---|---|---|
| Stn N | 12.8 | 6.3 | 8.3 ± 2.3 | Ref. 9 |
| SMB | 16.5 | 19.0 | 11.8 ± 5.8 | Ref. 10 |
| Average | 14.7 ± 2.6 | 12.7 ± 9.0 | | |

Calculated fluxes assume a fickian diffusion model[9] of $F_s = \phi D_{sed}(\Delta C_s/\Delta z)$, where $F_s$ is the flux of the solute of interest, $\phi$ is sediment porosity (0.90 and 0.96 $cm^3$ pore water $cm^{-3}$ sediment at 0–0.25 cm for station N and SMB, respectively), $D_{sed}$ is the sediment diffusion coefficient for each solute and is equal to $D_{sw}\phi^2$ (where $D_{sw}$, the diffusion coefficient in sea water, is conservatively estimated to be $1.5 \times 10^{-6}$ $cm^2\,s^{-1}$ for DOC[27,32] and $5.1 \times 10^{-6}$ $cm^2\,s^{-1}$ for $HCO_3^-$ (refs 13, 33) at both sites, irrespective of slight differences in bottom-water temperature of 1.5 and 5 °C for station N and SMB, respectively), $\Delta C_s$ is the difference in concentration of each solute between the shallowest sediment layer and the overlying sea water, and $\Delta z$ is the distance of the mid-point of the shallowest sediment layer from the sediment–water interface (0.125 cm). For calculated flux estimates, it was assumed that $DOC_{pw}$ concentrations were not affected by sampling artefacts due to pressure and temperature changes during core retrieval or by methodological constraints limiting the sectioning interval of sediments to 0.25 cm. Measured fluxes were determined *in situ* using benthic flux chambers[9,10].

from $CaCO_3$ ($\delta^{13}C = \sim 0$ to +1‰) dissolution (Table 1, Fig. 2). From pH profiles measured *in situ*[10] and our $DIC_{pw}$ profiles from both sites (Table 1), we have estimated that pore waters at Santa Monica basin reach saturation ($\Omega = 1.0$) with respect to calcite within 0.75 cm of the sediment–water interface and that significant $CaCO_3$ dissolution does not occur, similar to previously reported findings for the central basin[10]. These findings lead us to conclude that, to a first approximation, the change in $\delta^{13}C$ of $DIC_{pw}$ as a function of $DIC_{pw}$ concentration in sediments in

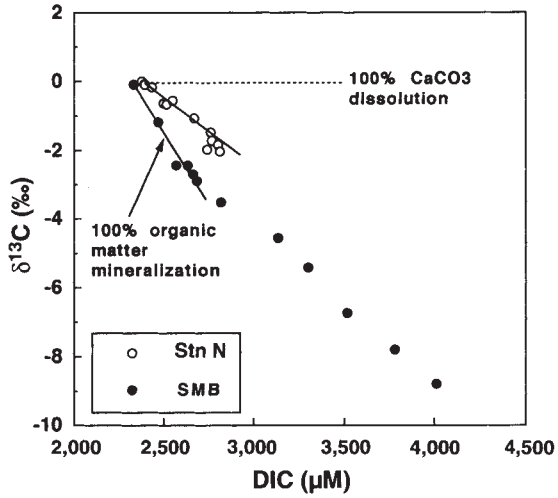


FIG. 2 Plot of $\delta^{13}C$ values of DIC versus concentration of DIC in pore water from station N and SMB. Regression of SMB $\delta^{13}C$ values as a function of DIC concentration from 0 to 1.5 cm depth ($n = 6$) yields $\Delta\delta^{13}C/[DIC] = -0.00787$, $r^2 = 0.9694$. For station N, $\Delta\delta^{13}C/[DIC] = -0.00370$ from 0 to 3 cm depth ($n = 9$), $r^2 = 0.9704$. It is assumed that SMB pore waters are saturated at all depths with respect to calcium carbonate, and that the change of $\delta^{13}C$ and DIC is due entirely to organic matter mineralization. The $\delta^{13}C$ of DIC at station N is calculated as being derived from an admixture of DIC from organic-matter mineralization (represented by the SMB regression) and $CaCO_3$ (0‰ with respect to $\delta^{13}C$) dissolution. The fraction of station N DIC derived from organic-matter mineralization is given by $F_{OM}(0.00787) + (1 - F_{OM}) = 0.0037$, where $F_{OM} = 0.47$.

Santa Monica basin can be attributed to organic-matter degradation alone. In contrast, station N pore waters are highly undersaturated ($\Omega = 0.5$–$0.8$) to at least 8 cm depth. A regression of $\delta^{13}C$ of $DIC_{pw}$ as a function of $DIC_{pw}$ concentration for both sites (Fig. 2) allows the fraction of DIC production from organic-matter degradation at station N to be calculated. Our estimate of 47% agrees closely with an independent estimate of 52 ± 7% made by comparing benthic fluxes of DIC to total organic-carbon degradation rates[9].

The $\Delta^{14}C$ values for $DIC_{pw}$ at Santa Monica basin are in all cases intermediate between the $\Delta^{14}C$ of SOC and $DOC_{pw}$, or SOC and $DIC_{olw}$ (Fig. 1*b*). Concentrations and $\Delta^{14}C$ values of $DIC_{pw}$ in excess of $DIC_{olw}$ concentrations and $\Delta^{14}C$ thus reflect inputs resulting from respiration of $DOC_{pw}$ and SOC at each relevant depth horizon. Assuming that the major sources of $DIC_{pw}$ are known and that to a first approximation bioturbation is negligible at this site, a mass balance for the $\Delta^{14}C$ of $DIC_{pw}$ is

$$\Delta^{14}C\text{-}DIC_{pw} = ([DIC_{olw}]/[DIC_{pw}])\Delta^{14}C\text{-}DIC_{olw} + (([DIC_{pw}] - [DIC_{olw}])/[DIC_{pw}])\Delta^{14}C_{source} \quad (1)$$

where subscript pw indicates pore water, subscript olw indicates sea water overlying sediments (also equivalent to pore water initially sequestered owing to sediment burial), ($[DIC_{pw}] - [DIC_{olw}]$) is the DIC added to pore waters due to the respiration of organic carbon, and $\Delta^{14}C_{source}$ is its radiocarbon signature. Using equation (1), we calculate that the source material of the DIC added to pore water has an average $\Delta^{14}C$ value of −55‰ at 2.5–3 cm depth and −85‰ at 5–6 cm depth. These values are more similar to $^{14}C$-enriched SOC than $^{14}C$-depleted $DOC_{pw}$ at Santa Monica basin (Table 1). In addition, selective mineralization of $^{14}C$-enriched components of either the bulk DOC or SOC may further result in the addition of $^{14}C$-enriched DIC to pore water.

A similar evaluation of the relative contribution of $DOC_{pw}$ and SOC to the $\Delta^{14}C$ values of $DIC_{pw}$ at station N is not possible at present because of uncertainties in the $\Delta^{14}C$ of the biogenic calcite raining to the sea floor. However, increasing divergence in the $\Delta^{14}C$ of $DIC_{pw}$ relative to the $DOC_{pw}$ and SOC pools with depth (that is, 10 cm; Fig. 1*a*) indicates that (1) $DIC_{pw}$ is unaffected by large changes in $\Delta^{14}C$ of SOC and $DOC_{pw}$ due to little net DIC addition below 3 cm (Table 1) or (2) selective mineralization of small amounts of 'young', downwardly mixed and isotopically distinct fractions of SOC and/or $DOC_{pw}$ may occur within the mixed layer of the sediment column.

The conspicuous concentration gradients of DOC and DIC across the sediment–water interface at both sites suggest that there are significant fluxes of these isotopically distinct solutes to the water column. Using a simplified fickian diffusion model (Table 2), we calculate fluxes (combined averages of both sites) to the overlying water column of 15 ± 3 $g\,C\,m^{-2}\,yr^{-1}$ for DOC and 13 ± 9 $g\,C\,m^{-2}\,yr^{-1}$ for DIC. The calculated DIC fluxes for both sites agree within measurement error with previously determined fluxes measured *in situ* using benthic flux chambers[9,10] (Table 2). Thus, reduced carbon in the form of DOC may be released back to the water column in amounts equal to fully mineralized carbon, representing an export of both carbon and energy from these sediments.

Porewater DOC at both sites was greatly enriched in $^{14}C$ relative to $DOC_{olw}$ (Fig. 1*a*, *b*; Table 1). The $\Delta^{14}C$ values of both DOC pools are expected to be more similar if pore water was a major source of DOC residing over the long term within the deep-water column, but elevated $\Delta^{14}C$ values of deep-ocean DOC have not been found[4,5,15]. We interpret these observations to indicate either that $^{14}C$-enriched $DOC_{pw}$ is not released from sediments in significant quantities or that it does not persist in the water column. One way that fluxes of DOC could potentially be overestimated by up to 1–3 orders of magnitude is by the microbial utilization of labile DOC at the oxygen- and nutrient-

rich sediment–water interface[16] (that is, narrower than the top 0–0.25 cm sampling interval); this would lead to a cross-interface DOC gradient that is smaller than that implied by our measurements (Table 1). Both the calculated and measured fluxes (Table 2) indicate that oxidation of $DOC_{pw}$ at the interface could potentially account for much of the DIC flux. Rapid utilization of $DOC_{pw}$ by water-column bacteria following its exchange would also diminish the presence of $DOC_{pw}$ in the water column.

Using average upper water column mixed-layer DOC concentrations of 60 μM and deep-water concentrations of 40 μM (refs 4, 5), the inventory of DOC from 0–4,000 m in an area such as station N is 2,200 g C $m^{-2}$. If $DOC_{pw}$ persists in the water column, our upper estimate of sediment–water DOC flux of 15 g C $m^{-2}$ $yr^{-1}$ leads to a lower estimated replacement time of $\geqslant$150 yr. Lower flux rates would lead to greater replacement times. Current and previous estimates[4,15,16] of the average apparent $^{14}C$ age of water-column DOC below ~1,000 m depth in different regions of the North Pacific are ~6,000 yr. Although pore water may be a significant source of DOC to sea water, our findings indicate that sediments are unlikely to provide preaged DOC to the oceans, thus limiting the strength of this source over the long term ($10^3$–$10^4$ yr). Instead, the DOC supplied by sediments to ocean waters must be relatively young and, in a manner similar to its $^{14}C$-enriched riverine counterpart[3,17–19], ages and undergoes degradation within the ocean itself. □

Received 24 August 1994; accepted 13 January 1995.

1. Emerson, S. & Hedges, J. I. *Paleoceanography* **3,** 621–634 (1988).
2. Berner, R. A. & Canfield, D. E. *Am. J. Sci.* **289,** 333–361 (1989).
3. Hedges, J. I. *Mar. Chem.* **39,** 67–93 (1992).
4. Williams, P. M. & Druffel, E. R. M. *Nature* **330,** 246–248 (1987).
5. Druffel, E. R. M., Williams, P. M., Bauer, J. E. & Ertel, J. R. *J. geophys. Res.* **97,** 15639–15659 (1992).
6. Bauer, J. E., Haddad, R. I. & Des Marais, D. J. *Mar. Chem.* **33,** 335–351 (1991).
7. Bauer, J. E., Spies, R. B., Vogel, J. S., Nelson, D. E. & Southon, J. R. *Nature* **348,** 230–232 (1990).
8. McCorkle, D. C. & Emerson, S. R. *Geochim. cosmichim. Acta* **52,** 1169–1178 (1988).
9. Reimers, C. E., Jahnke, R. A. & McCorkle, D. C. *Globl biogeochem. Cycles* **6,** 199–224 (1992).
10. Jahnke, R. A. *J. mar. Res.* **48,** 413–436 (1990).
11. Berger, R., Taylor, I. E. & Libby, W. F. *Science* **153,** 864–866 (1966).
12. Trumbore, S. E., Schiff, S. L., Aravena, R. & Elgood, R. *Radiocarbon* **34,** 626–635 (1992).
13. McCorkle, D. C., Emerson, S. R. & Quay, P. D. *Earth planet. Sci. Lett.* **74,** 13–26 (1985).
14. McNichol, A. P., Lee, C. & Druffel, E. R. M. *Geochim. cosmochim. Acta* **52,** 1531–1543 (1988).
15. Bauer, J. E., Williams, P. M. & Druffel, E. R. M. *Nature* **357,** 667–670 (1992).
16. Jahnke, R. A., Craven, D. B. & Gaillard, J.-F. *Geochim. cosmochim. Acta* **58,** 2799–2809 (1994).
17. Maybeck, M. *Am. J. Sci.* **282,** 401–450 (1982).
18. Meyers-Schulte, K. J. & Hedges, J. I. *Nature* **321,** 61–63 (1986).
19. Hedges, J. I. *et al. Science* **231,** 1129–1131 (1986).
20. Smith, K. L., Baldwin, R. J. & Williams, P. M. *Nature* **359,** 313–316 (1992).
21. Smith, K. L., Kaufman, R. S. & Baldwin, R. J. *Limnol. Oceanogr.* **39,** 1101–1118 (1994).
22. Cai, W.-J. Thesis, Univ. California (1992).
23. Shaw, T. *et al. Geochim. cosmochim. Acta* **54,** 1233–1246 (1990).
24. Cai, W.-J., Reimers, C. & Shaw, T. *Geochim. cosmochim. Acta* (in the press).
25. Bruland, K., Bertine, K., Koide, M. & Goldberg, E. D. *Envir. Sci. Technol.* **8,** 425–432 (1974).
26. Finney, B. P. & Huh, C.-A. *Envir. Sci. Technol.* **23,** 294–303 (1989).
27. Martin, W. R. & McCorkle, D. C. *Limnol. Oceanogr.* **38,** 1464–1479 (1993).
28. Williams, P. M., Bauer, J. E., Robertson, K. J., Wolgast, D. M. & Occelli, M. L. *Mar. Chem.* **41,** 271–281 (1993).
29. Sofer, Z. *Analyt. Chem.* **52,** 1389–1391 (1980).
30. Stuiver, M. & Polach, H. A. *Radiocarbon* **19,** 355–363 (1977).
31. Vogel, J. S., Nelson, D. E. & Southon, J. R. *Radiocarbon* **29,** 323–333 (1987).
32. Burdige, D. J., Alperin, M. J., Homstead, J. & Martens, C. S. *Geophys. Res. Lett.* **19,** 1851–1854 (1992).
33. Li, Y.-H. & Gregory, S. G. *Geochim. cosmochim. Acta* **20,** 131–140 (1974).

ACKNOWLEDGEMENTS. We thank J. Southon, S. Trumbore and M. Kashgarian for assistance with $\Delta^{14}C$ analyses; S. Griffin and D. Wolgast for help with sample preparation; J. Hedges, J. Chanton and W. Martin for comments and suggestions; and the crew of the RV *New Horizon* for help with sample collection and ship logistics. This work was supported by the US NSF.

# Explosive fragmentation of erupting magma

**Ichiro Sugioka*† & Marcus Bursik‡**

* Graduate Aeronautics Laboratory, California Institute of Technology, Pasadena, California 91125, USA
‡ Department of Geology, State University of New York at Buffalo, Buffalo, New York 14260, USA

**THE magma responsible for explosive volcanic eruptions has both a volatile and an inert phase. Deep in the conduit of an active volcano, bubbles nucleate as the volatiles exsolve[1–3]. As the magma rises, the bubbles grow through depressurization and continued exsolution. It is thought that when the pressure in the bubbles exceeds that in the overlying material, the magma undergoes a rapid transformation from a continuous magmatic phase with bubbles to a continuous gas phase with fragmented pyroclastic material[1,2]. The fragmentation process is complex and poorly understood. To understand better how the transport of fragmented material is coupled to exsolution and vaporization, we have performed depressurization experiments on a two-phase system, designed to simulate the eruption process. We identify a new explosive vaporization process, in which a fragmentation front propagates downwards through a mixture of volatile liquid and inert particulate material, suppressing the growth of nucleated bubbles by compressing the material ahead of it. This process is distinct from, and may complement, previously identified fragmentation mechanisms such as non-nucleate vaporization[4] and fragmentation induced by an expanding magmatic foam[5].**

Because of the violence of the explosive process, conditions in an active volcanic conduit are not amenable to direct observation. In addition, the thermodynamics and fluid dynamics controlling the flux of mass, momentum and energy are closely coupled and nonlinear[2]. In magmatic eruptions, the volatile phase consists of water, $CO_2$ and other less-abundant dissolved components[6], whereas the inert phase consists of a viscous silicate liquid, crystals and country rock. In the experiments (Fig. 1), vapour was rapidly produced by the sudden depressurization of a volatile liquid within a matrix of (inert) spherical particles. The two phases are analogous to the separate volatile and inert phases in erupting magma. Because the phases were intermingled, they were most like mechanically mixed magma and volatiles, as may occur in hydrovolcanic[7] or magmatic[8] systems. The particles not only served as the material to be fragmented and transported, but also provided bubble nucleation sites virtually identical to the crystal surfaces that perform this role in natural melts[3]. Both settings involve the nucleation and growth of bubbles by depressurization and diffusion, and the subsequent transport of material by the released vapour. The process of vaporization in the experiments is an analogue for exsolution and vaporization in explosive eruptions. Depressurization below the vapour pressure of a volatile liquid is equivalent to instantaneously and uniformly superheating it[4], and is analogous to supersaturating a dissolved phase. The experiments were performed with different volatile components and different dump-tank pressures to simulate differences in saturation vapour pressure, and hence volatile content in magma. A centrifuge was used to simulate magma columns up to 50 m deep, and quasi-steady eruption conditions lasting for several seconds[9,10]. By transformation into the reference frame of a rising magma, steady phenomena were probably simulated.

The vaporization of the volatile liquid is a thermodynamic process that converts the internal energy of the fluid into the kinetic energy of fragmentation and expulsion. The change in energy, $\Delta I$, is initiated by depressurization at constant temperature, $\Delta P$, and is given by $\Delta I = v\Delta P$ where $\Delta P = P_v - P_d$, the volatile vapour pressure minus the ambient, dump-tank (back)

† Present address: Volvo Monitoring and Concept Center, 700 Via Alondra, Camarillo, California 93012, USA.